The Plant Cell, Vol. 25: 2545–2559, July 2013, www.plantcell.org © 2013 American Society of Plant Biologists. All rights reserved.

Folate Polyglutamylation Is Involved in Chromatin Silencing by Maintaining Global DNA Methylation and Histone H3K9 Dimethylation in *Arabidopsis*[C][W]

Hao-Ran Zhou,[a,b,1] Fang-Fang Zhang,[a,1] Ze-Yang Ma,[a] Huan-Wei Huang,[a] Ling Jiang,[c] Tao Cai,[a] Jian-Kang Zhu,[d,e] Chuyi Zhang,[c] and Xin-Jian He[a,b,2]

[a] National Institute of Biological Sciences, Beijing 102206, China
[b] Graduate School of Peking Union Medical College, Beijing 100730, China
[c] Biotechnology Research Institute, Chinese Academy of Agricultural Sciences, Beijing 100081, China
[d] Shanghai Center for Plant Stress Biology and Institute of Plant Physiology and Ecology, Shanghai Institutes for Biological Sciences, Chinese Academy of Sciences, Shanghai 200032, China
[e] Department of Horticulture and Landscape Architecture, Purdue University, West Lafayette, Indiana 47907

ORCID ID: 0000-0002-2878-7461 (X-J. H.).

DNA methylation and repressive histone Histone3 Lysine9 (H3K9) dimethylation correlate with chromatin silencing in plants and mammals. To identify factors required for DNA methylation and H3K9 dimethylation, we screened for suppressors of the *repressor of silencing1* (*ros1*) mutation, which causes silencing of the expression of the *RD29A* (RESPONSE TO DESSICATION 29A) promoter-driven luciferase transgene (*RD29A-LUC*) and the *35S* promoter-driven *NPTII* (NEOMYCIN PHOSPHOTRANSFERASE II) transgene (*35S-NPTII*). We identified the folylpolyglutamate synthetase FPGS1 and the known factor DECREASED DNA METHYLATION1 (DDM1). The *fpgs1* and *ddm1* mutations release the silencing of both *RD29A-LUC* and *35S-NPTII*. Genome-wide analysis indicated that the *fpgs1* mutation reduces DNA methylation and releases chromatin silencing at a genome-wide scale. The effect of *fpgs1* on chromatin silencing is correlated with reduced levels of DNA methylation and H3K9 dimethylation. Supplementation of *fpgs1* mutants with 5-formyltetrahydrofolate, a stable form of folate, rescues the defects in DNA methylation, histone H3K9 dimethylation, and chromatin silencing. The competitive inhibitor of methyltransferases, *S*-adenosylhomocysteine, is markedly upregulated in *fpgs1*, by which *fpgs1* reduces *S*-adenosylmethionine accessibility to methyltransferases and accordingly affects DNA and histone methylation. These results suggest that FPGS1-mediated folate polyglutamylation is required for DNA methylation and H3K9 dimethylation through its function in one-carbon metabolism. Our study makes an important contribution to understanding the complex interplay among metabolism, development, and epigenetic regulation.

INTRODUCTION

In plants and mammals, DNA methylation at 5-position of cytosine is an important chromatin feature that is involved in transposon silencing, genome stability, and gene regulation (Slotkin and Martienssen, 2007; Matzke et al., 2009; Law and Jacobsen, 2010; He et al., 2011). DNA methylation is highly correlated with the repressive histone Histone3 Lysine9 dimethylation (H3K9me2) mark at heterochromatic regions. In *Arabidopsis thaliana*, DNA methylation is present in all three cytosine contexts, which include symmetric CG and CHG sites and asymmetric CHH sites. CG methylation is maintained by the homolog of human DNA METHYLTRANSFERASE1 (MET1) (Ronemus et al., 1996). DECREASED DNA METHYLATION1 (DDM1), a SWItch2/Sucrose NonFermentable2 (SWI2/SNF2) chromatin-remodeling protein, is required for maintaining CG methylation as well as H3K9me2 (Jeddeloh et al., 1999). CHG methylation is catalyzed by a plant-specific CHROMOMETHYLASE3 (CMT3) and depends on H3K9me2 (Cao and Jacobsen, 2002; Du et al., 2012). The direct binding of CMT3 to H3K9me2-containing nucleosomes is required for the interplay between DNA methylation and H3K9me2 (Du et al., 2012). CHH methylation is mainly established by DOMAINS REARRANGED METHYLTRANSFERASE2 (DRM2) and its homologs through the RNA-directed DNA methylation (RdDM) pathway (Henderson et al., 2010). In *Arabidopsis*, histone H3K9 dimethylation is catalyzed by the *Drosophila melanogaster* SUPPRESSOR OF VARIEGATION3-9 (SU[VAR]3-9) homologs and related proteins (Baumbusch et al., 2001; Law and Jacobsen, 2010; Veiseth et al., 2011). All these proteins contain a catalytic SET domain. Additionally, an extra SRA (SET- or RING-associated) methyl binding domain is present at the N termini of SU(VAR)3-9 homologs (Baumbusch et al., 2001). The 5-methyl-cytosine binding ability of the SRA domain is required for both DNA methylation and H3K9me2 (Rajakumara et al., 2011). The cooperation between DNA methylation and histone methylation is essential for maintaining stable chromatin silencing in *Arabidopsis* (Baubec et al., 2010).

S-adenosylmethionine (SAM) serves as the universal methyl-group donor for methyltransferases including DNA and histone

[1] These authors contributed equally to this work.
[2] Address correspondence to hexinjian@nibs.ac.cn.
The author responsible for distribution of materials integral to the findings presented in this article in accordance with the policy described in the Instructions for Authors (www.plantcell.org) is: Xin-Jian He (hexinjian@nibs.ac.cn).
[C] Some figures in this article are displayed in color online but in black and white in the print edition.
[W] Online version contains Web-only data.
www.plantcell.org/cgi/doi/10.1105/tpc.113.114678

methyltransferases (Loenen, 2006; Zhang et al., 2012). SAM originates from folate-dependent one-carbon metabolism. The vitamin B12-dependent methionine (Met) synthase uses 5-methyl-tetrahydrofolate (5-CH3-THF) as the methyl-group donor for the methylation of homocysteine (Hcy) to Met, the precursor of SAM (Friso et al., 2002). After transfer of the methyl group, SAM is converted to *S*-adenosylhomocysteine (SAH), which is a strong inhibitor of methyltransferases. Removal of SAH is critical to avoid the inhibitory effect of SAH on methylation reactions (Molloy, 2012). *S*-adenosylhomocysteine hydrolase (SAHH) is the enzyme responsible for the conversion of SAH to Hcy and adenosine. Hcy is further recycled for Met and then SAM biosynthesis (Molloy, 2012). Partial inactivation of SAHH by antisense RNA in tobacco (*Nicotiana tabacum*) causes morphological changes and DNA hypomethylation (Tanaka et al., 1997). The *SAHH/HOMOLOGY-DEPENDENT GENE SILENCING1* (*HOG1*) knockout mutants in *Arabidopsis* are embryo lethal, whereas the weak *hog1* alleles are leaky and result in genome demethylation (Rocha et al., 2005). In *Arabidopsis*, the *hog1/sahh1* mutants were recovered from several independent forward genetic screens, which suggested that HOG1/SAHH1 plays a critical role in development as well as in DNA and histone methylation and epigenetic silencing (Rocha et al., 2005; Mull et al., 2006; Wu et al., 2009; Baubec et al., 2010; Ouyang et al., 2012). The weak reduction in SAM/SAH ratio is likely correlated with the effect of *hog1* on DNA methylation (Rocha et al., 2005).

Tetrahydrofolate and its derivatives act as cofactors in one-carbon metabolism and are required for the transfer of one-carbon units during the synthesis of purines, thymidylate, pantothenate, formyl-methionyl tRNA, and Met (Cossins and Chen, 1997; Lucock, 2000). Met is the direct precursor of SAM, which is required for methylation of DNA, RNA, and proteins. Folates are comprised of pterin, paminobenzoic acid, and Glu moieties. In vivo, folates can be polyglutamylated by sequential conjugation of additional *r*-linked Glu residues to the first Glu by folylpolyglutamate synthetase (Ravanel et al., 2001). Plants synthesize folates, but mammals must obtain folates from exogenous sources. Therefore, inadequate folate intake in mammals impairs folate-dependent processes and causes several abnormalities, including embryonic defects, neural tube defects, cardiovascular disease, and cancers (Molloy, 2012). The influence of folate status on DNA methylation has been demonstrated in mammals (Giovannucci et al., 1993; Friso et al., 2002). DNA hypomethylation may be one of the important molecular bases for the abnormalities caused by folate deficiency. The methylenetetrahydrofolate reductase catalyzes the conversion of 5,10-methylene THF to 5-methyl THF and plays a central role in folate-mediated one-carbon metabolism (Frosst et al., 1995). An extensively studied polymorphism (C677T) in the enzyme is correlated with DNA hypomethylation and uracil misincorporation when folate intake is inadequate, and C677T may increase the risk of folate deficiency-related abnormalities (Frosst et al., 1995; Shelnutt et al., 2004). The function of folate in DNA and histone methylation in plants was recently demonstrated in *Arabidopsis* (Zhang et al., 2012). However, further studies are required to fully understand the regulatory mechanism of folate and its role in DNA and histone methylation in vivo.

In our genetic system, both the *RD29A* (*RESPONSE TO DESSICATION29A*) promoter-driven luciferase transgene (*RD29A-LUC*) and the *35S* promoter-driven *NPTII* (*NEOMYCIN PHOSPHOTRANSFERASE II*) transgene (*35S-NPTII*) are silenced by mutations in the DNA glycosylase/demethylase REPRESSOR OF SILENCING1 (ROS1) (Gong et al., 2002). We identified a number of components required for transcriptional silencing by screening for suppressors of *ros1* based on both luminescence imaging and kanamycin resistance (He et al., 2011; Liu and Gong, 2011). The results showed that RdDM is responsible for the silencing of *RD29A-LUC* (He et al., 2009), whereas DNA replication and repair proteins are required for maintaining the silencing of *35S-NPTII* (Liu and Gong, 2011). The function of DNA replication and repair proteins in transcriptional silencing involves repressive histone H3K9 dimethylation but not DNA methylation (Liu and Gong, 2011). The histone H2B deubiquitination enzyme UBIQUITIN-SPECIFIC PROTEASE 26 (UBP26) and HISTONE DEACETYLASE 6 (HDA6) are required for the silencing of both transgenes (Sridhar et al., 2007; He et al., 2009). In this study, we examined the mechanisms of epigenetic regulation by screening for mutants that release the *ros1*-based silencing of two transgenes. We identified DDM1, which is known to be important for both DNA methylation and histone H3K9 dimethylation, and also identified FOLYLPOLYGLUTAMATE SYNTHETASE 1 (FPGS1). Our examination of the *fpgs1* mutants suggests that folate polyglutamylation plays a key role in the regulation of methyl-group supply for global DNA and histone methylation.

RESULTS

Identification of Suppressors of *ros1*

Our genetic screening system uses an *Arabidopsis ros1* mutant line that harbors two silenced reporter genes: the *RD29A* promoter-driven luciferase gene (*RD29A-LUC*) and the *35S* promoter-driven *NPTII* (*35S-NPTII*) (Gong et al., 2002). Suppressors of *ros1* can be identified by their increased luciferase expression and kanamycin resistance resulting from a release of the *ros1* silencing of these two transgenes. Here, by screening for suppressors of *ros1*, we identified a *ddm1* mutant in the *ros1* background (see Supplemental Figure 1 online). The silencing of both *RD29A-LUC* and *35S-NPTII* was released by the *ddm1* mutation (Figures 1A and 1B), suggesting that DDM1 has a universal role in transcriptional silencing. Moreover, we identified an additional suppressor, which we identified as *fpgs1*, based on our subsequent characterization (see below) (Figure 1A). The silencing of both *Rd29A-LUC* and *35S-NPTII* was released in *fpgs1* as well as in *ros1 ddm1* (Figure 1A). The effect of *fpgs1* on the silencing of *RD29A-LUC* was less than that of *ddm1*. In *Arabidopsis*, many endogenous genes, transposable elements (TEs), and DNA repeats are silenced by DNA methylation and repressive histone modifications. The DNA repeats flanked protein-coding gene *SDC* (*SUPPRESSOR OF DRM1 DRM2 CMT3*), and the TEs At-*MU1* and At-*GP1* are

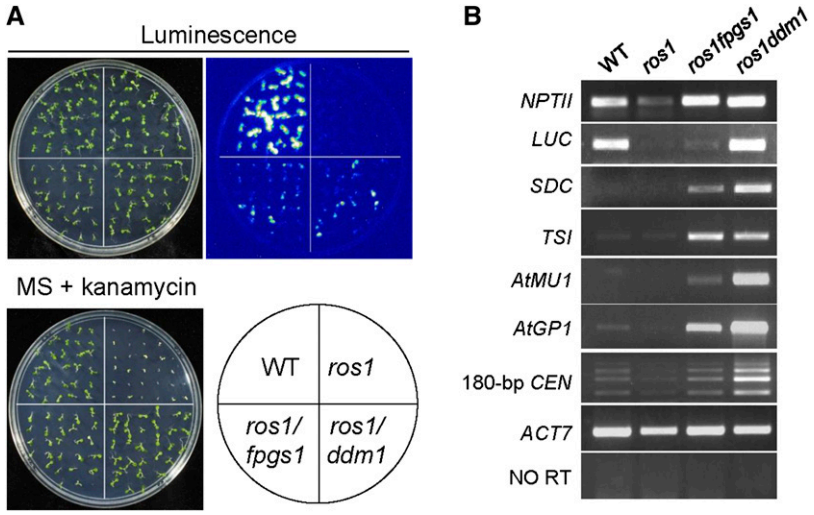

Figure 1. The Silencing of Transgenes and Endogenous Genomic Sequences Was Released in Both *ros1 fpgs1* and *ros1 ddm1* Mutants.

(A) The silencing of *RD29A-LUC* and *35S-NPTII* transgenes was released in *ros1 fpgs1*and *ros1 ddm1*. The *LUC* and *NPTII* expression levels were evaluated based on luminescence imaging and kanamycin resistance, respectively. The kanamycin resistance of seedlings was determined by growing the seedlings on MS medium supplemented with 150 mg/L kanamycin. The wild type (WT) and *ros1* were used as controls.
(B) The transcript levels of indicated loci were examined by RT-PCR. The actin gene *ACT7* was amplified as an internal control. "NO RT" indicates the amplification of *ACT7* when RNA was used as template without reverse transcription.
[See online article for color version of this figure.]

canonical targets of RdDM (Henderson and Jacobsen, 2008; He et al., 2009), whereas *TRANSCRIPTIONALLY SILENT INFORMATION* (*TSI*) is the repetitive DNA sequence targeted by DNA replication and repair proteins but not by RdDM components (Xia et al., 2006). The 180-bp centromeric DNA repeats are not affected by RdDM components or DNA replication and repair proteins (Xia et al., 2006; He et al., 2009b; Yin et al., 2009). Our RT-PCR results indicated that all these endogenous silenced loci are upregulated by *ddm1* and to a lesser extent by *fpgs1* (Figure 1B). Moreover, the effect of *fpgs1* on transcriptional silencing of *35S-NPTII*, *SDC*, *TSI*, At-*MU1*, and At-*GP1* was confirmed by quantitative RT-PCR (see Supplemental Figure 2 online). The results suggest that both *fpgs1* and *ddm1* mutations have a universal effect on chromatin silencing.

DNA Methylation and Histone H3K9 Dimethylation Are Reduced in the *fpgs1* Mutant

We evaluated the effect of the *fpgs1* mutation on DNA methylation by bisulfite sequencing and DNA gel blotting. Bisulfite sequencing suggested that the DNA methylation levels at both the *35S-NPTII* transgene promoter and the *RD29A-LUC* transgene promoter were reduced by *fpgs1* but that the effect of *fpgs1* was less than that of *ddm1* (Figures 2A and 2B; see Supplemental Table 1 online). Similarly, the DNA methylation level at the endogenous *RD29A* promoter was reduced by *ddm1* and to a lesser extent by *fpgs1* (see Supplemental Figure 3A and Supplemental Table 1 online). Both *ddm1* and *fpgs1* affect DNA methylation in all three cytosine contexts, including CG, CHG, and CHH sites, but the effect of *fpgs1* is generally weaker than that of *ddm1* (Figures 2A and 2B; see Supplemental Table 1 online). The effect of *fpgs1* and *ddm1* on DNA methylation at endogenous genomic loci was determined by DNA gel blotting. The results indicated that at the three tested genomic loci (180-bp centromeric DNA repeats, *TSI*, and *5S rDNA*), the CG methylation as determined by *Hpa*II cleavage was mildly reduced by *fpgs1* and was drastically reduced by *ddm1* (Figure 2C). The CHG methylation determined by *Msp*I cleavage was reduced by *ddm1* and to a lesser extent by *fpgs1* (see Supplemental Figure 3B online). The cytosine methylation at asymmetric CHH sites was not affected by *fpgs1* at the 180-bp centromeric DNA repeats, *5S rDNA*, and *TSI* (see Supplemental Figure 3B online). Although the CHH methylation at the 180-bp centromeric DNA repeats and *TSI* sites was also not affected by *ddm1*, the CHH methylation at 5S rDNA was clearly upregulated by *ddm1* (see Supplemental Figure 3B online). This promoting effect of *ddm1* on CHH methylation was consistent with the previous finding that the *ddm1* mutation induces de novo DNA methylation through the RdDM pathway (Teixeira et al., 2009).

We conducted immunoblotting assays to determine whether the *fpgs1* mutation impairs the different types of repressive histone methylation, including histone H3K9 monomethylation (H3K9me1), H3K9 dimethylation (H3K9me2), and Histone3 Lysine27 monomethylation (H3K27me1) (Johnson et al., 2008; Roudier et al., 2011). As expected, all the three types of repressive histone methylation were reduced by the *ddm1* mutation in *ros1ddm1* (Figure 2D). Moreover, the H3K9me2 level in *ros1 fpgs1* was clearly reduced, while the levels of H3K9me1 and H3K27me1 in *ros1 fpgs1* were comparable to that in the wild type and *ros1* (Figure 2D).

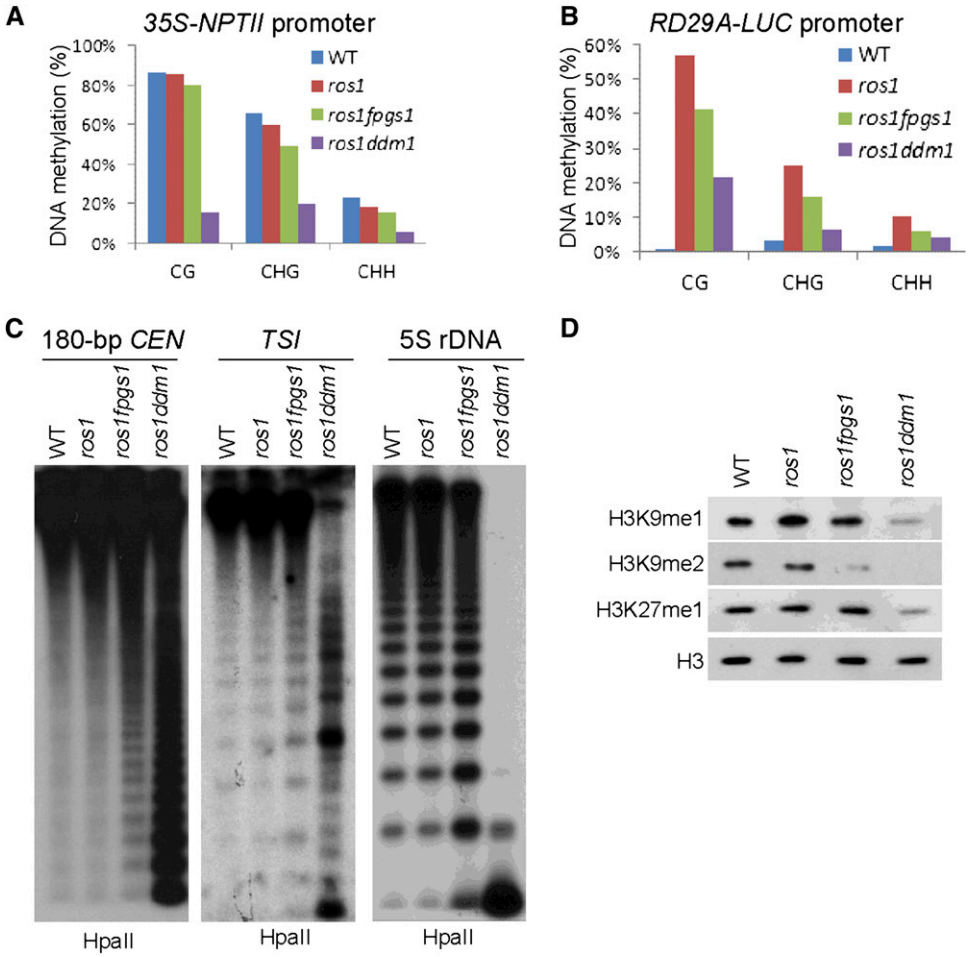

Figure 2. The Effect of *fpgs1* and *ddm1* on DNA and Histone Methylation.

(A) and **(B)** Detection of DNA methylation at the promoters of *35S-NPTII* and *RD29A-LUC* transgenes by bisulfite sequencing. The DNA methylation levels at CG, CHG, and CHH sites are shown. WT, the wild type.

(C) The DNA methylation of 180-bp centromeric DNA, *TSI*, and *5S rDNA* was evaluated by DNA gel blotting. Genomic DNA was cleaved by the DNA methylation-sensitive endonuclease *Hpa*II followed by DNA gel blotting.

(D) The overall levels of H3K9me1, H3K9me2, and H3K27me1 determined by immunoblotting. The protein extracts were isolated from the wild type, *ros1*, *ros1 fpgs1*, and *ros1 ddm1*. The H3 signal was detected as a loading control.

Map-Based Cloning and Characterization of *FPGS1*

We identified the crucial mutation in *ros1 fpgs1* by map-based cloning. The mutant was crossed to the *ros1* mutant (Salk_045303) in the Columbia-0 background, and the F2 plants were selected for map-based cloning based on visualization of luminescence and kanamycin resistance. The mutation was localized to an ~432-kb interval on chromosome 5 (see Supplemental Figure 4A online). A G-to-A mutation in *FPGS1* was identified in *ros1 fpgs1* by sequencing candidate genes in the region. The mutation in *FPGS1* disrupts the splicing donor site in the eleventh intron of *FPGS1* (see Supplemental Figure 4B online). We performed RT-PCR using the primers flanking the eleventh intron to test whether the *FPGS1* transcript is affected by *fpgs1* (see Supplemental Figures 5A to 5C online). The results indicated that two abnormal *FPGS1* transcripts are present in *ros1 fpgs1*, whereas the normal *FPGS1* transcript identified in the wild type and *ros1* is absent in *ros1 fpgs1* (see Supplemental Figure 5A online). Sequencing of the two abnormal *FPGS1* transcripts demonstrated that one transcript retains the full length of the eleventh intron and the other transcript retains a part of the intron (see Supplemental Figures 5B and 5C online). The reading frame shifts in both abnormal *FPGS1* transcript variants, suggesting that the functional *FPGS1* transcript is disrupted by the *fpgs1* mutation in *ros1 fpgs1*.

The full-length *FPGS1* genomic sequence was constructed and transformed into the *ros1 fpgs1* mutant for complementation testing. Seedling growth assay showed that the root growth mutant is significantly retarded in *ros1 fpgs1* compared with that in the wild type and *ros1* (see Supplemental Figure 6A online), which is consistent with the morphological phenotype of *fpgs1* as reported previously (Srivastava et al., 2011). We found that

the defective root growth of *ros1 fpgs1* was complemented by the *FPGS1* transgene (see Supplemental Figure 6A online). Moreover, our results demonstrated that the silencing of *RD29A-LUC* as well as of *35S-NPTII* is restored by the *PFGS1* transgene in the *ros1 fpgs1* background (see Supplemental Figure 6B online). Because the silencing of endogenous genomic target loci At-*GP1* and *TSI* is released by *fpgs1* (Figure 1B), we tested whether the *FPGS1* transgene restores the silencing of the two loci by RT-PCR. The results demonstrated that both At-*GP1* and *TSI* are silenced by the *FPGS1* transgene in *ros1 fpgs1* (see Supplemental Figure 6C online). These results suggest that *FPGS1* is not only required for root growth but also for transcriptional silencing.

FPGS1 encodes a conserved folylpolyglutamate synthetase isoform that catalyzes folate polyglutamylation on the initial Glu of folate in chloroplasts (Ravanel et al., 2001; Mehrshahi et al., 2010; Srivastava et al., 2011). To confirm the function of FPGS1 in DNA methylation, we determined the DNA methylation levels of At-*GP1* and *TSI* in two individual *fpgs1* T-DNA mutants, Salk_015472 and Salk_007791 (see Supplemental Figure 7A online). The results indicated that DNA methylation of At-*GP1* and *TSI* is markedly decreased in the two individual *fpgs1* mutants relative to the wild type (see Supplemental Figure 7B online), confirming that FPGS1 is required for DNA methylation. The At-*GP1* and *TSI* transcript levels were determined by RT-PCR (see Supplemental Figure 7C online). The results showed that transcriptional silencing of At-*GP1* and *TSI* is significantly released in the two *fpgs1* T-DNA mutants. These results confirm that FPGS1 is required for DNA methylation and transcriptional silencing. *Arabidopsis* has three folylpolyglutamate synthetases, FPGS1, FPGS2, and FPGS3 (Mehrshahi et al., 2010). The *fpgs2* and *fpgs3* T-DNA mutants, Salk_008883 and SAIL_580_H10, were used to determine the possible function of FPGS2 and FPGS3 in DNA methylation by chop-PCR (see Supplemental Figure 7A online). In chop-PCR, genomic DNA from each genotype was digested by the methylated DNA-specific restriction enzyme *Mcr*BC, followed by quantitative PCR; therefore, an increased signal in chop-PCR indicates lower levels of methylation. The results suggested that the DNA methylation levels of At-*GP1* and *TSI* were not affected by *fpgs2* and *fpgs3* (see Supplemental Figure 7B online). Moreover, we tested the effect of *fpgs2* and *fpgs3* on transcriptional silencing of At-*GP1* and *TSI* by RT-PCR and found that neither *fpgs2* nor *fpgs3* affects transcriptional silencing (see Supplemental Figure 7C online), which is consistent with the finding that *fpgs2* and *fpgs3* have no effect on DNA methylation at the loci (see Supplemental Figure 7B online). These results imply that either FPGS2 or FPGS3 is dispensable for DNA methylation and transcriptional silencing, but functional redundancy between FPGS2 and FPGS3 cannot be excluded.

Genome-Wide Effect of *fpgs1* on DNA Methylation

We conducted whole-genome bisulfite sequencing to analyze the global effect of *fpgs1* on DNA methylation. The effect of *ddm1* on DNA methylation was evaluated as a control. From the whole-genome bisulfite sequencing, we obtained 11,323,625, 14,196,929, and 9,592,891 unique mapped ~40-nucleotide reads for *ros1*, *ros1 ddm1*, and *ros1 fpgs1*, respectively (see Supplemental Table 2 online). Calculations of the average CG, CHG, and CHH methylation across the whole genome indicated that the DNA methylation at all the three cytosine contexts is reduced by *ddm1* and to a lesser extent by *fpgs1* (Table 1). To evaluate the quality of the whole-genome bisulfite sequencing results, we checked the DNA methylation levels of the *35S-NPTII* and *RD29A-LUC* promoters determined by the whole-genome bisulfite sequencing (see Supplemental Figures 8A and 8B online). The effect *fpgs1* and *ddm1* on DNA methylation of the *35S-NPTII* and *RD29A-LUC* promoters as determined by the whole-genome bisulfite sequencing was highly similar to the effect that was determined by sequence-specific bisulfite sequencing (Figures 2A and 2B; see Supplemental Figures 8A and 8B online), suggesting the whole-genome bisulfite sequencing generated high-quality data.

Table 1. Average Cytosine Methylation Levels at CG, CHG, and CHH and Total Cytosine Sites.

Genotypes	CG	CHG	CHH	Total
ros1	18.40%	5.30%	1.70%	4.85%
ros1 fpgs1	15.60%	3.10%	1.30%	3.73%
ros1 ddm1	8.00%	1.80%	1.00%	2.23%

The average CG, CHG, and CHH methylation was determined at genes and TEs, respectively. Consistent with previous reports (Wierzbicki et al., 2012), our result suggested that gene body methylation was predominantly present at CG sites (Figure 3A). Gene body CG methylation was clearly reduced by *ddm1* as well as by *fpgs1*. At the regions surrounding gene bodies, CG methylation was clearly reduced by *ddm1* but only marginally reduced by *fpgs1*, whereas CHG and CHH methylation was reduced by *ddm1* as well as by *fpgs1* (Figure 3A). In contrast with genes, TE bodies showed higher DNA methylation than their surrounding regions at CG, CHG, and CHH sites (Figure 3B). Not only *ddm1* but also *fpgs1* drastically reduced TE body methylation at all the three cytosine contexts, although the effect of *fpgs1* is less than *ddm1* (Figure 3B). At TE surrounding regions, *ddm1* causes a decrease of DNA methylation at CG, CHG, and CHH sites, but *fpgs1* can only affect DNA methylation at CHG and CHH sites (Figure 3B). The effects of *fpgs1* on DNA methylation across *Arabidopsis* chromosomes indicated that *fpgs1* reduces CHG and CHH methylation substantially at centromeric and pericentromeric regions and weakly at euchromatic regions. However, the effect of *fpgs1* on CG methylation is always weak throughout whole *Arabidopsis* chromosomes, which is different from the substantial effects of *ddm1* on all cytosine contexts at centromeric and pericentromeric regions (see Supplemental Figures 9A to 9J online).

The number of differentially methylated genes and TEs was determined; loci were selected that showed a significant ($P < 0.05$) change of more than 1.5-fold compared with the control *ros1* plants (see Supplemental Data Sets 1 to 4 online). The results indicated that 2946 genes and 1549 TEs are hypomethylated at CG sites in *fpgs1* mutants, compared with 6330 genes and 8897 TEs that are hypomethylated in *ddm1* mutants (Figure 3C). In all, 45.8% of hypomethylated genes (1350/2946) and 52.8% of TEs (818/1549) caused by *fpgs1* at CG sites are

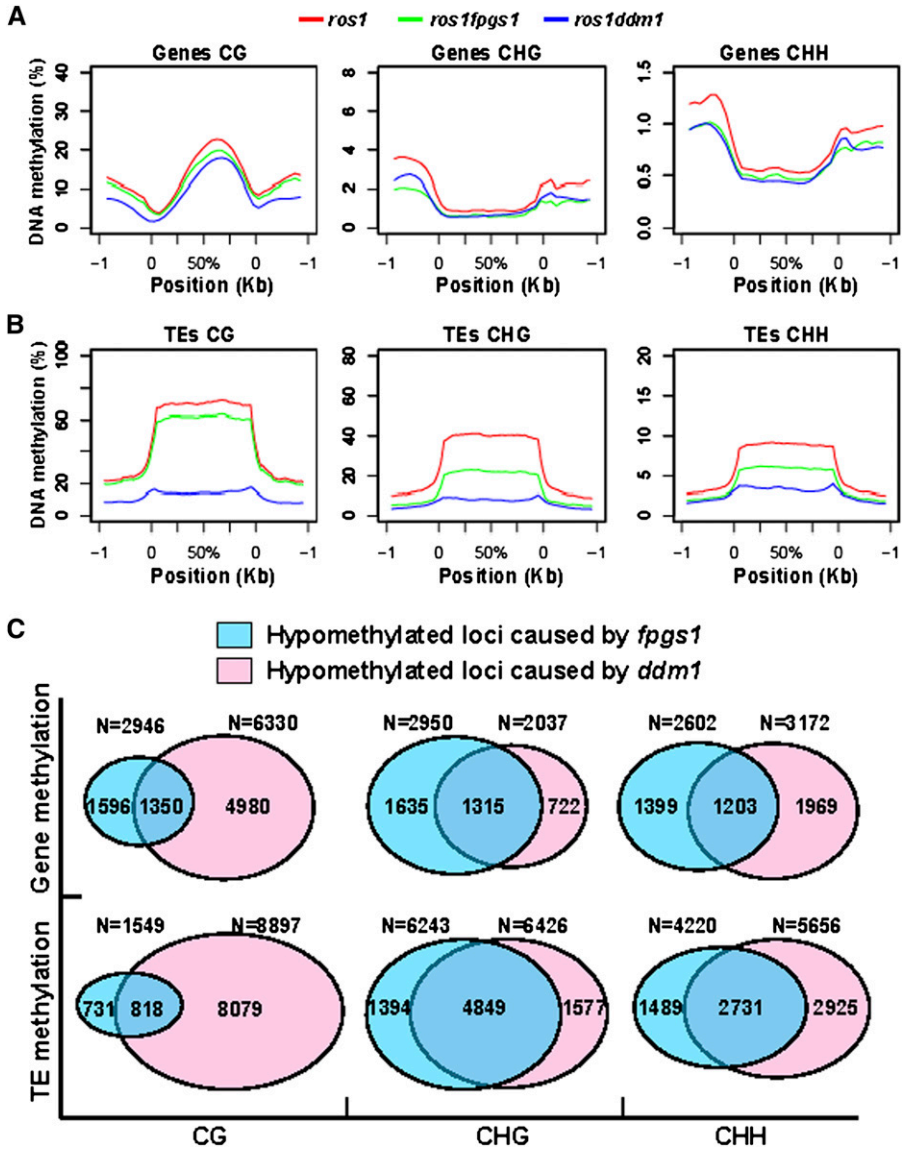

Figure 3. The Effect of *fpgs1* and *ddm1* on DNA Methylation at Genes and TEs.

(A) and **(B)** Diagrams show the levels of CG, CHG, and CHH methylation at genes **(A)**, TEs **(B)**, and their 1-kb upstream and downstream regions in *ros1* (read line), *ros1 fpgs1* (green line), and *ros1 ddm1* (blue line).

(C) Shown are the numbers of hypomethylated genes and TEs caused by *fpgs1* and *ddm1* as well as the numbers of their overlapping loci. The numbers of hypomethylated loci at CG, CHG, and CHH sites are separately indicated.

also hypomethylated by *ddm1* (Figure 3C), whereas 21.3% of *ddm1*-mediated hypomethylated genes (1350/6330) and 9.2% of TEs (818/8897) at CG sites are simultaneously affected by *fpgs1*. The numbers of hypomethylated genes and TEs at CHG sites caused by *fpgs1* are 2950 and 6243, respectively. Among them, 1315 genes and 4849 TEs are also hypomethylated by *ddm1* at CHG sites (Figure 3C). The numbers of hypomethylated genes and TEs at CHH sites caused by *fpgs1* are comparable to those caused by *ddm1* (Figure 3C). There are 2602 genes and 4220 TEs that are hypomethylated in *ros1 fpgs1* at CHH sites, compared with 3172 genes and 5656 TEs that are hypomethylated in *ros1 ddm1* (Figure 3C). Among them, 1203 genes and 2731 TEs are overlapped between *ros1 fpgs1* and *ros1 ddm1* (Figure 3C), suggesting that the CHH sites in a large number of genes and TEs are common targets of FPGS1 and DDM1. Together, FPGS1 generally contributes to DNA methylation in all three cytosine contexts, including CG, CHG, and CHH sites.

Genome-Wide Effect of *fpgs1* on Chromatin Silencing

We performed RNA deep sequencing to detect the genome-wide effect of *fpgs1* on chromatin silencing. We obtained 60,999,740

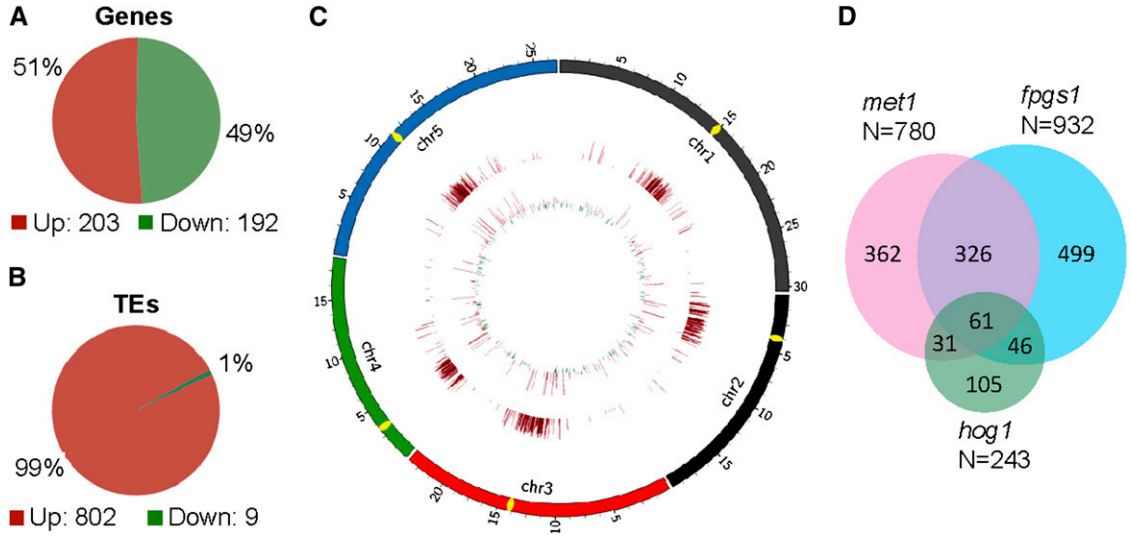

Figure 4. Characterization of FPGS1-Dependent Loci by RNA Deep Sequencing.

(A) and **(B)** Diagrams show the numbers of differentially expressed protein-coding genes **(A)** and TEs **(B)** caused by *fpgs1*.
(C) The distribution of differentially expressed protein-coding genes and TEs caused by *fpgs1*. The transcript levels of genes and TEs are shown in the inside circle and the outside circle, respectively. The outward bars and inward bars represent *fpgs1*-upregulated loci and -downregulated loci, respectively. The lengths of bars represent the fold changes of differences.
(D) The *fpgs1*-upregulated Arabidopsis Genome Initiative annotated genes and transposons were compared with the previously reported *met1*- and *hog1*-upregulated loci. The numbers of the upregulated loci as well as the number of overlapping loci are shown.

~40-nucleotide RNA reads for *ros1* and 58,592,351 for *ros1 fpgs1*. More than 90% of these RNA reads can be uniquely matched on the *Arabidopsis* genome, suggesting the high quality of the RNA libraries (see Supplemental Table 3 online). By comparing the RNA data between *ros1* and *ros1 fpgs1*, we found that 395 protein-coding genes and 811 TEs were significantly affected by *fpgs1*. The numbers of upregulated versus downregulated genes in *ros1 fpgs1* relative to *ros1* were similar (203 upregulated versus 192 downregulated) (Figure 4A; see Supplemental Data Set 5 online). However, the number of upregulated TEs (802) was much higher than the number of downregulated TEs (9) (Figure 4B; see Supplemental Data Set 6 online). From the diagram of the genome-wide effect of *fpgs1* on RNA transcript levels, we found that protein-coding genes are equivalently affected by *fpgs1* throughout chromosomes (Figure 4C). However, the TEs induced by *fpgs1* are enriched in the centromeric and pericentromeric regions (Figure 4C), which is consistent with the distribution of TEs on chromosomes. The results suggest that TEs rather than genes are preferentially silenced by FPGS1-dependent mechanisms.

Our RNA deep sequencing identified a total of 932 annotated genes and transposons that are upregulated by *fpgs1* (see Supplemental Data Set 7 online). Two previous reports demonstrated that MET1 and HOG1 are required for the silencing of a number of annotated genes and transposons, including 780 loci upregulated by *met1* and 243 loci upregulated by *hog1* (To et al., 2011; Ouyang et al., 2012). In the loci upregulated by *met1* and *hog1*, 387 (49.6% of 780) and 107 (44.0% of 243) loci, respectively, overlap with the loci upregulated by *fpgs1* (Figure 4D). The rates of overlapping loci are significantly higher than expected by chance (P = 0 for the overlap between *met1* and *fpgs1*; P < 3.65e-91 for the overlap between *hog1* and *fpgs1*). The results demonstrated that FPGS1-dependent silencing shares a number of common targets with MET1 and HOG1 at the whole-genome level, suggesting that like MET1 and HOG1, FPGS1 is probably required for maintaining DNA methylation and chromatin silencing at the whole-genome level. The identified upregulated loci were confirmed by quantitative RT-PCR (see Supplemental Figure 10 online), suggesting that the RNA deep sequencing results are reliable.

The Effect of *fpgs1* on TE Silencing Is Correlated with DNA Methylation

We analyzed the genome-wide effect of *fpgs1* on DNA methylation and RNA transcripts, respectively. To determine whether the effect of *fpgs1* on DNA methylation and RNA transcripts is correlated, we analyzed the DNA methylation status of those differentially expressed genes and TEs caused by *fpgs1*. From the RNA deep sequencing data, the number of upregulated genes (203) caused by *fpgs1* is equivalent to the number of downregulated genes (192) (Figure 4A). We calculated the overall DNA methylation levels of upregulated genes, downregulated genes, and all genes (Figure 5A). The results indicated that the DNA methylation level of upregulated genes is slightly higher than that of downregulated genes as well as of all genes whether *FPGS1* is mutated or not, and the *fpgs1* mutation has no much effect on DNA methylation at all genes (Figure 5A). Our RNA deep sequencing data suggested that the number of upregulated TEs (802) caused by *fpgs1* is much more than the

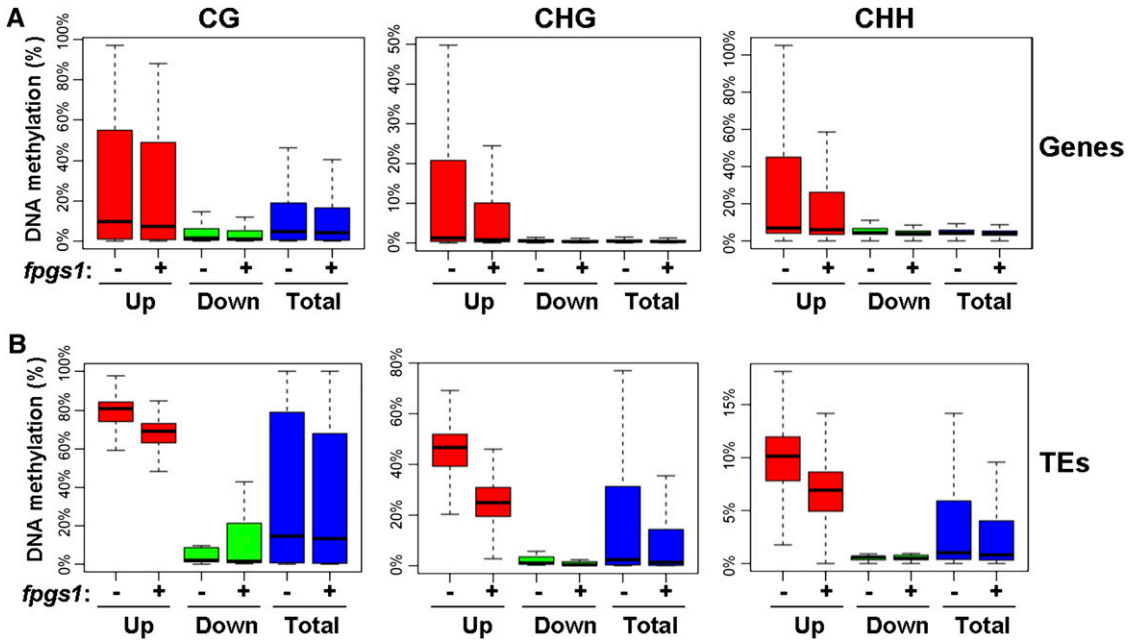

Figure 5. Box Plot of DNA Methylation Levels in *fpgs1*-Mediated Differentially Expressed Genes and TEs.

DNA methylation of differentially expressed genes **(A)** and TEs **(B)** in *ros1* and *ros1fpgs1*. "−", *ros1*; "+", *ros1 fpgs1*. "Up" and "Down" represent genes or TEs that are upregulated and downregulated by *fpgs1*, respectively. "Total" represents total genes or TEs in *Arabidopsis*. DNA methylation at CG, CHG, and CHH sites was separately indicated.
[See online article for color version of this figure.]

number of downregulated TEs (9) (Figure 4B). Our whole-genome DNA methylation analysis indicated that the overall DNA methylation level of upregulated TEs is much higher than that of downregulated TEs and all TEs (Figure 5B), suggesting that the hypermethylated TEs are preferentially affected by *fpgs1*. Moreover, the DNA methylation level of the upregulated TEs is markedly reduced by *fpgs1* at all the three cytosine contexts CG, CHG, and CHH (Figure 5B). These results demonstrated that the role of FPGS1 in TE silencing is affected with its function in DNA methylation.

5-formyltetrahydrofolate Complements the Defect of Chromatin Silencing Caused by *fpgs1*

Previous studies showed that mutation of *FPGS1* significantly reduced total folate abundance (especially in chloroplasts) and led to short primary roots (Mehrshahi et al., 2010; Srivastava et al., 2011). Exogenous application of 5-formyltetrahydrofolate (5-CHO-THF), a stable form of folate, could rescue the root defect as well as the other developmental defects of the *fpgs1* mutant (Srivastava et al., 2011). We investigated whether application of 5-CHO-THF complements the defects in chromatin silencing caused by *fpgs1*. A root growth assay indicated that the roots of *ros1 fpgs1* plants are much shorter than the wild type and *ros1* on Murashige and Skoog (MS) medium without extra supplementation (Figure 6A). The root defect of *ros1 fpgs1* was mostly complemented by supplementation with 250 μM 5-CHO-THF to the MS medium (Figure 6A). We next examined the effect of 5-CHO-THF on kanamycin resistance of *ros1 fpgs1* mutant plants. Because the silencing of the *35S-NPTII* transgene is released by the *fpgs1* mutation in *ros1 fpgs1* (Figures 1B and 6B; see Supplemental Figures 2 and 6 online), the *ros1 fpgs1* mutant plants are resistant to 150 mg/L kanamycin on MS medium (Figures 1A and 6A). However, the kanamycin resistance of *ros1 fpgs1* was markedly reduced when 250 μM 5-CHO-THF was supplemented in MS medium (Figure 6A). Quantitative RT-PCR demonstrated that addition of 5-CHO-THF specifically suppressed *35S-NPTII* transgene expression in *ros1 fpgs1* but had no effect on the wild type or *ros1* (see Supplemental Figure 2 online).

We further checked whether supplementation with 5-CHO-THF could also restore the silencing of endogenous genomic loci that is released in *ros1 fpgs1*. The silencing of *SDC*, *TSI*, At-*MU1*, At-*GP1*, and the 180-bp centromeric DNA repeats was suppressed in *ros1 fpgs1* on MS control medium, but the silencing of all these loci was restored when 5-CHO-THF was added to the medium (Figure 6B; see Supplemental Figure 2 online). These results suggest that the chromatin silencing defect in *ros1 fpgs1* can be complemented by exogenous application of 5-CHO-THF. Our RNA deep sequencing analysis identified a number of TEs that are upregulated by *fpgs1* (Figure 4B). By quantitative RT-PCR, we found that the high transcript levels of these TEs caused by *fpgs1* were markedly decreased when 5-CHO-THF was added to MS medium (see Supplemental Figure 10 online). The folate derivative may restore the chromatin silencing of *ros1 fpgs1* at the whole-genome level.

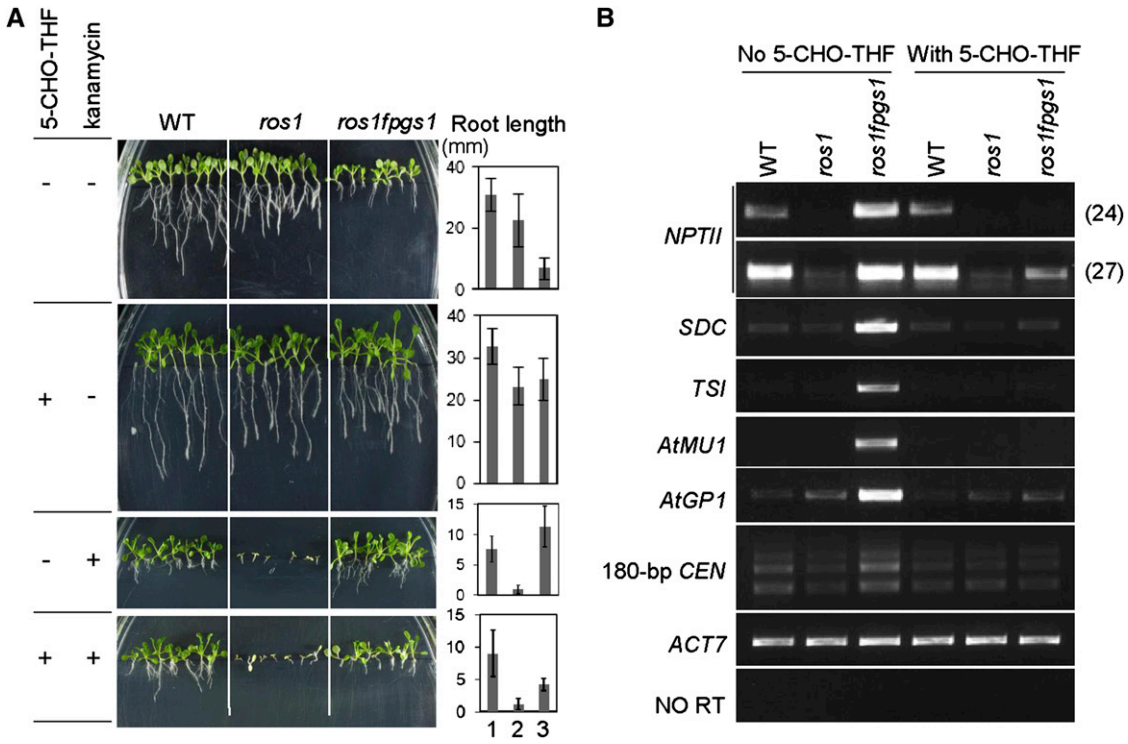

Figure 6. Exogenous Application of 5-CHO-THF Rescues the Defect in Chromatin Silencing.

(A) Addition of 250 μM 5-CHO-THF complements the short root phenotype of *ros1 fpgs1* on MS medium and compromises the kanamycin resistance of *ros1fpgs1* on MS medium supplemented with 150 mg/L kanamycin. The MS medium that contains or does not contain the indicated reagents is indicated by "+" and "−," respectively. Root length for each sample is shown in the right panel. 1, 2, and 3 represent the wild type (WT), *ros1*, and *ros1 fpgs1*, respectively.

(B) Exogenous application of 5-CHO-THF rescues the defect in chromatin silencing in *ros1 fpgs1*. The transcript levels of the indicated loci were evaluated by RT-PCR. *ACT7* was amplified as an internal control.

[See online article for color version of this figure.]

5-CHO-THF Complements the Defects of DNA Methylation and Histone H3K9 Dimethylation Caused by *fpgs1*

Because DNA methylation is reduced by *fpgs1* (Figures 2 and 3; see Supplemental Figures 3 and 9 online), we tested whether the silencing defect of *ros1 fpgs1* at the loci identified by RNA deep sequencing is affected with the reduction of DNA methylation. By using the unmethylated DNA-sensitive endonuclease *Mcr*BC followed by chop-PCR, we found that DNA methylation was drastically reduced by *fpgs1* at the newly identified loci upregulated by *fpgs1* (Figure 7A; see Supplemental Figure 11 online). We tested whether exogenous application of 5-CHO-THF complements the defect of DNA methylation in *ros1 fpgs1* in vivo. Our chop-PCR results showed that the DNA methylation defect was markedly rescued by application of 5-CHO-THF at the loci identified by RNA deep sequencing (Figure 7A; see Supplemental Figure 11 online). Moreover, DNA gel blotting assays indicated that the reduction of DNA methylation at the 180-bp centromeric DNA and *TSI* was partially rescued by 5-CHO-THF (see Supplemental Figure 12 online). Therefore, exogenous application of 5-CHO-THF complements the defects of DNA methylation caused by *fpgs1*. Previous studies indicated that the total folate level is significantly reduced by *fpgs1* (Mehrshahi et al., 2010; Srivastava et al., 2011). A proper level of folate is likely required for maintaining DNA methylation in vivo. The role of FPGS1 in the maintenance of DNA methylation is related to its function in folate metabolism. Moreover, we found that even in wild-type plants, application of 5-CHO-THF increases DNA methylation at AT1TE45380, AT1TE45390. AT2G20460, and AT5G41660 (Figure 7A), suggesting that the folate-mediated one-carbon metabolism may act as a limiting factor for maintaining DNA methylation during the development of wild-type plants.

We demonstrated the effect of *fpgs1* on histone H3K9 dimethylation (Figure 2D). By immunofluorescence assays, we investigated whether 5-CHO-THF can complement the defect of histone H3K9me2 caused by *fpgs1*. Without 5-CHO-THF treatment, 65.4% of nuclei show condensed H3K9me2 signals in *ros1 fpgs1*, which is significantly less than the 84.1% in the wild type and the 85.7% in *ros1* (Figures 7B and 7C), suggesting that *fpgs1* reduces H3K9 dimethylation in vivo. However, the effect of *fpgs1* on H3K9 dimethylation is much less than that of *ddm1* because the percentage of nuclei that show condensed H3K9 dimethylation signals was reduced to 11.5% in *ros1 ddm1* (Figures 7B and 7C).

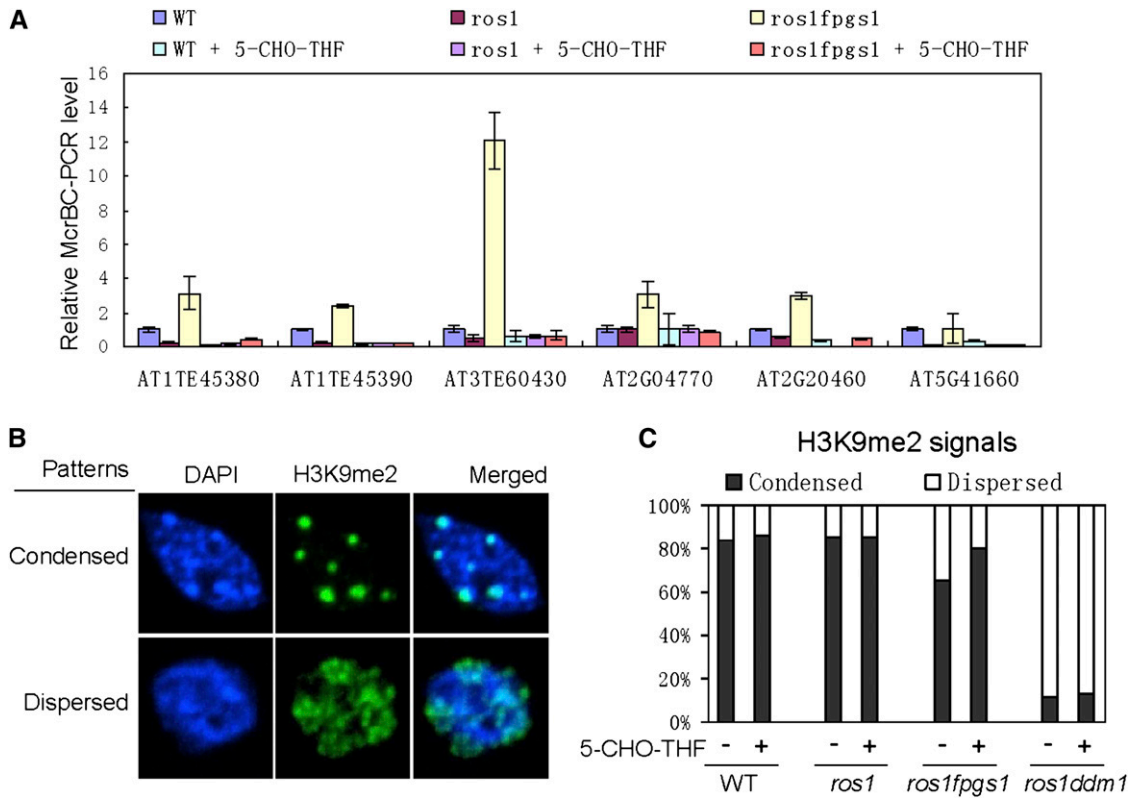

Figure 7. Effect of 5-CHO-THF on DNA Methylation and Histone H3K9 Dimethylation.

(A) Genomic DNA was cleaved by the unmethylated DNA-sensitive endonuclease *Mcr*BC followed by quantitative PCR. DNA methylation was evaluated at the identified *fpgs1*-upregulated genes and TEs in the wild type (WT), *ros1*, and *ros1 fpgs1*. 5-CHO-THF (500 μM) was added to MS medium to determine the effect of 5-CHO-THF on DNA methylation. Relative PCR levels and standard deviations are shown in the chart.

(B) Shown are the nuclei that have condensed H3K9me2 signals and dispersed H3K9me2 signals. The nuclei were counterstained by 4′,6-diamidino-2-phenylindole (DAPI).

(C) The percentages of the nuclei with condensed and dispersed H3K9me2 signals are separately indicated for the wild type, *ros1*, and *ros1 fpgs1*. The effect of 5-CHO-THF on the H3K9me2 signals is shown.

When 5-CHO-THF was applied, the percentage of nuclei showing condensed H3K9me2 signals was increased to 80.0% in *ros1 fpgs1*, whereas the percentages of such nuclei in the wild type, *ros1*, and *ros1 ddm1* were not significantly affected (Figures 7B and 7C). The results indicated that application of 5-CHO-THF specifically rescued the defect of H3K9me2 caused by *fpgs1*. Examining these data together, we conclude that the functioning of FPGS1 in folate metabolism is required for both DNA methylation and H3K9 dimethylation in vivo.

The *fpgs1* Mutation Causes Accumulation of Hcy and SAH

Folate-mediated one-carbon metabolism produces SAM, the universal methyl-donor required for the methylation of DNA, RNA, and proteins. In one-carbon metabolism, 5-CH3-THF is the methyl donor for Met. Met synthase catalyzes the transfer of one methyl-group from 5-CH3-THF to Hcy to form Met, which is then converted to SAM by Met adenosyltransferase. SAM is converted to SAH after its methyl-group is transferred to substrates. SAH can compete with SAM to bind to the active site of methyltransferases (Molloy et al., 2012). It is possible that *fpgs1* affects DNA methylation by disrupting one-carbon metabolism. We measured SAM and its related metabolites SAH, Hcy, Met, and Cys in the *fpgs1*T-DNA mutant, SALK_015472, as well as in the wild type. The results indicated that SAH and Hcy are markedly upregulated in *fpgs1* compared with that in the wild type, whereas Met, Cys, and SAM are not significantly affected in *fpgs1* (Figure 8A). The high levels of SAH and Hcy were restored to the wild-type levels when the *FPGS1* transgene was expressed in *fpgs1* (Figure 8A), indicating that *fpgs1* is responsible for upregulation of SAH and Hcy.

Folate polyglutamination directly affects one-carbon metabolism because various folate-dependent enzymes in the one-carbon metabolism preferentially utilize polyglutamated folate rather than monoglutamated folate (Shane, 1989; Ravanel et al., 2001). Moreover, folate polyglutamation prevents the transfer of folate between different cellular compartments, which may be critical for the regulation of specific folate-mediated metabolism in the compartments (Matherly and Goldman, 2003). Given that DNA methylation is markedly reduced by *fpgs1*, it is possible

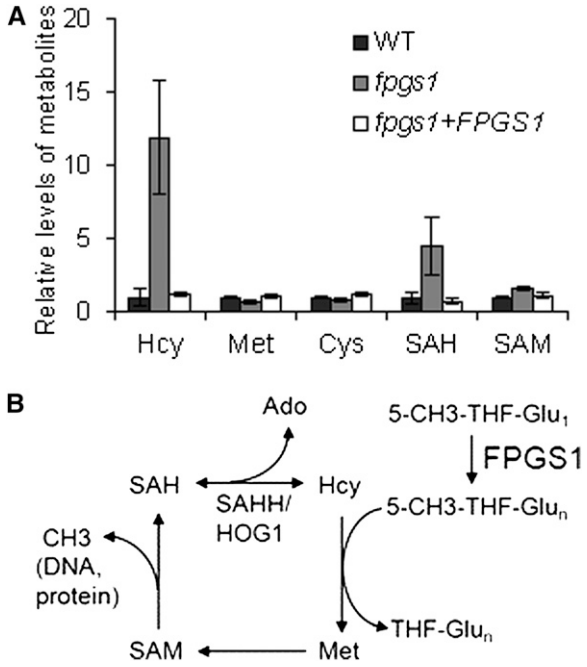

Figure 8. The *fpgs1* Mutation Causes Accumulation of Hcy and SAH and Reduces SAM Accessibility to DNA Methyltransferases.

(A) The metabolites related to one-carbon metabolism were tested in the wild type (WT), the *fpgs1* T-DNA mutant SALK_015472, and the *FPGS1* transgenic plants in the *fpgs1* mutant background. Standard deviation of three independent biological repeats is shown.

(B) Model for the function of FPGS1 on methyl-group supply in one-carbon metabolism. FPGS1 converts 5-CH3-THF-Glu_1 to 5-CH3-THF-Glu_n, which can transfer its active methyl group to Hcy for Met synthesis. Met are converted to SAM, which can act as a cofactor to provide methyl-group for many methyltransferases. SAH is the product of methylation reaction and is a competitor inhibitor of methyltransferases. SAHH can be cleaved by SAH hydrolase (SAHH1/HOG1) to generate adenosine (Ado) and Hcy.

that 5-CH3-THF can be utilized as a methyl-group donor only when it is polyglutamated (Figure 8B). The induction of Hcy caused by *fpgs1* is likely caused by a feedback effect of the reduced level of polyglutamated 5-CH3-THF. The high level of Hcy is easily converted to SAH and results in SAH accumulation in *fpgs1* (Figures 8A and 8B). SAH can compete with SAM and act as a competitive inhibitor of DNA methyltransferases. Thus, the high level of SAH caused by *fpgs1* is directly related to the reduction of DNA methylation.

DISCUSSION

Folate and its derivatives are crucial for the homeostasis of the one-carbon pool. Plants, fungi, and bacteria can synthesize folate, but mammals must take up exogenous folate. In humans, folate deficiency is related to DNA hypomethylation and uracil misincorporation and causes diverse abnormalities (Giovannucci et al., 1993; Molloy, 2012). Therefore, studying the crucial enzymes in folate metabolism is important for understanding the role folate metabolism in humans as well as in plants and other organisms.

In *Arabidopsis*, folylpolyglutamate synthetases have three members, FPGS1, FPGS2, and FPGS3, which are present in the chloroplast, mitochondria, and cytosol, respectively (Ravanel et al., 2001). However, the functions of the three FPGS proteins are redundant and can be partially rescued by each other (Mehrshahi et al., 2010). The *fpgs1* mutant was previously identified based on its morphological phenotypes (Srivastava et al., 2011). The primary root of the *fpgs1* mutant is significantly shorter than the wild type (Srivastava et al., 2011). The *fpgs2* and *fpgs3* single mutants have no obvious morphological phenotypes, but the *fpgs2 fpgs3* double mutant exhibits seedling lethality (Mehrshahi et al., 2010). Moreover, the *fpgs1 fpgs2* double mutant is embryo-lethal, and the *fpgs1 fpgs3* double mutant causes more severe morphological defects than the *fpgs1* single mutant, with dwarfed leaves, late flowering, and reduced fertility (Mehrshahi et al., 2010). These results underscore the essential role of folate polyglutamylation in *Arabidopsis*. Although the importance of folate polyglutamylation in *Arabidopsis* development has been demonstrated, the mechanism by which folate polyglutamylation affects gene expression and development remains to be elucidated.

We identified the folylpolyglutamate synthetase FPGS1 by screening for suppressors of *ros1* and demonstrated that FPGS1 is required for DNA and histone methylation and chromatin silencing. *HOG1/SAHH1* encodes an SAHH that catalyzes the conversion of SAH to Hcy, which is further utilized for Met and then SAM synthesis. Moreover, because SAH is a strong competitive inhibitor of methyltransferases, removal of SAH by SAHH is also critical for the activity of methyltransferases (Bacolla et al., 1999; Rocha et al., 2005). In *Arabidopsis*, the *hog1/sahh1* mutations suppress DNA methylation and transcriptional silencing (Rocha et al., 2005; Mull et al., 2006; Baubec et al., 2010; Ouyang et al., 2012). Moreover, the *hog1* mutant also shows developmental abnormalities, including delayed germination, slow growth, short primary roots, and reduced fertility (Rocha et al., 2005; Wu et al., 2009). These developmental phenotypes are highly similar to the phenotypes found in the previously described *fpgs1 fpgs3* double mutant (Mehrshahi et al., 2010). It is possible that the developmental phenotypes of *fpgs1 fpgs3* and *hog1* might be related to the global defects in DNA methylation and chromatin silencing. In comparing *fpgs1*-upregulated loci with the *hog1*-upregulated loci reported previously (Ouyang et al., 2012), we found that 107 loci are upregulated by both *fpgs1* and *hog1*, which is significantly greater than expected by chance. Upregulation of these loci might account for the developmental defects caused by both *fpgs1* and *hog1*.

Our RNA deep sequencing suggested that the *fpgs1* mutation releases the silencing of a number of TEs (Figure 4B). We observed that TEs are predominantly upregulated by *fpgs1*, whereas the number of upregulated versus downregulated genes caused by *fpgs1* is similar (Figures 4A and 4B). Upregulation of TEs is highly correlated with reduced DNA methylation in *ros1fpgs1* relative to *ros1*, whereas upregulation of genes is not significantly correlated with DNA methylation changes caused by *fpgs1* (Figures 5A and 5B). The results suggest that the effect of *fpgs1* on transcriptional silencing of TEs is directly through its effect on DNA methylation. By contrast, the effect of

fpgs1 on differentially expressed genes is mostly independent of DNA methylation changes.

Our genome-wide bisulfite sequencing indicated that the *fpgs1* mutation reduces DNA methylation especially at centromeric and pericentromeric regions on each *Arabidopsis* chromosome (see Supplemental Figure 9 online). Because TEs are predominantly present at centromeric and pericentromeric regions, the derepression effect of *fpgs1* on TEs relates to the reduction of DNA methylation at the whole-genome level. Moreover, we found that the *fpgs1* mutation upregulates and downregulates similar numbers of protein-coding genes, although *fpgs1* predominantly upregulates TEs. However, the upregulation of protein-coding genes is significantly stronger in centromeric and pericentromeric regions than in the two arms of chromosomes (Figure 4C), which is consistent with the stronger effect of *fpgs1* on the DNA methylation at centromeric and pericentromeric regions (see Supplemental Figure 9 online). Our genome-wide bisulfite sequencing indicated that the average DNA methylation level at the promoter regions of protein-coding genes is markedly reduced by *fpgs1* especially at CHG and CHH sites (Figure 3A), supporting that the derepression effect of *fpgs1* on the genes in centromeric and pericentromeric regions is related to the reduction of DNA methylation at their promoter regions.

The effect of *fpgs1* on DNA methylation and chromatin silencing is less than that of *ddm1* (Figures 1B, 2A to 2C, 3A, 3B, and 4; see Supplemental Figure 9 online). In *Arabidopsis*, the chloroplast, the mitochondrion, and the cytosol each has one kind of folylpolyglutamate synthetase, FPGS1, FPGS2, and FPGS3, respectively (Ravanel et al., 2001). The weak effect of *fpgs1* is probably due to a functional redundancy between FPGS1 and its homologs FPGS2 and FPGS3 (Ravanel et al., 2001). A previous study indicated that the *fpgs1 fpgs2*, *fpgs1 fpgs3*, and *fpgs2 fpgs3* double mutants have much more severe developmental defects than any of the single mutants, suggesting that FPGS1, FPGS2, and FPGS3 can partially replace each other (Mehrshahi et al., 2010). Although the effect of *fpgs2* and *fpgs3* on DNA methylation and transcriptional silencing was not found in each single mutant (see Supplemental Figures 7B and 7C online), we cannot exclude that FPGS2 and FPGS3 may function redundantly in DNA and histone methylation and transcriptional silencing.

During *Arabidopsis* development, DNA methylation at symmetric cytosine sites CG and CHG can be maintained by the DNA methyltransferases MET1 and CMT3, respectively, whereas unsymmetric CHH methylation can be established on unmethylated DNA by the DNA methyltransferase DRM2 and its homologs (Ronemus et al., 1996; Cao and Jacobsen, 2002; Henderson et al., 2010). Our study indicated that the DNA methylation defect at symmetric CG and CHG sites caused by *fpgs1* can be rescued by application of 5-CHO-THF, suggesting that DNA methylation at symmetric cytosine sites can be immediately established even if the cytosine in parent cells is unmethylated. The results revealed that DNA methylation can be effectively reestablished during development, which is in contrast with previous findings that disruption of DNA methylation caused by *ddm1* can only be gradually complemented after several generations (Teixeira et al., 2009). We found that the overall DNA methylation level is higher in the *fpgs1* mutant than in *ddm1*, although both *fpgs1* and *ddm1* significantly reduced DNA methylation at the genome-wide level (Table 1, Figures 2A to 2C). It is possible that the relatively higher basal DNA methylation level in the *fpgs1* mutant enables exogenous 5-CHO-THF to rapidly restore DNA methylation to the wild-type level.

Our results suggest that the defect of folate polyglutamylation caused by *fpgs1* affects folate-mediated one-carbon metabolism (Figure 8A). One-carbon metabolism is required for the biosynthesis of SAM, a crucial methyl-group donor for methylation of DNA, histone, and other substrates (Loenen, 2006). SAH is a competitive inhibitor of methyltransferases and reduces the accessibility of SAM to methyltransferases. A proper SAM/SAH ratio is required for the activity of methyltransferases (Molloy, 2012). Our results suggest that SAH is drastically induced by *fpgs1*, which results in a low level of SAM/SAH ratio (Figure 8A). Different cytosine contexts and histone methyl marks are catalyzed by diverse DNA and histone methyltransferases. We hypothesize that the sensitivity of various DNA and histone methyltransferases to SAM/SAH reduction is different. In the *fpgs1* mutant, the reduction of SAM/SAH can only effectively affect a subset of DNA and histone methyltransferases, leading to reduced DNA and histone methylation at the part of cytosine contexts and histone marks. Alternatively, it is also possible that histone H3K9 dimethylation is indirectly affected by the reduction of DNA methylation caused by *fpgs1* because of the coupling of DNA methylation and H3K9 dimethylation ((Rajakumara et al., 2011; Du et al., 2012). Future studies are needed to understand this preferential effect of folate polyglutamylation on DNA methylation and H3K9 dimethylation.

METHODS

Plant Materials, Mutant Identification, and Cloning

Arabidopsis thaliana C24 and its derivative *ros1* mutant that harbors the *RD29A-LUC* and *35S-NPTII* transgenes were used in this study. We mutagenized the *ros1* mutant seeds with ethyl methanesulfonate to screen for suppressors of *ros1* as previously described (Liu et al., 2011). The selfed T2 seedlings were screened based on luminescence imaging or kanamycin resistance. The positive mutants were confirmed based on the luminescence strength and kanamycin resistance of their offspring. The confirmed mutant was crossed to the *ros1* mutant in the Columbia-0 background (Salk_045303), and the selfed F2 population was used for map-based cloning to localize the chromosome region of the mutation. The candidate genes of the region were sequenced to find the mutation. The *FPGS1* genomic sequence was cloned into the modified pCAMBIA1305 vector with its 3′-terminal in frame with the 3xFlag epitope sequence. The primers used for *FPGS1* cloning are indicated in Supplemental Data Set 8 online. The construct was transformed into *ros1 pfgs1* for complementation testing.

Analysis of RNA Transcript Levels

We performed quantitative RT-PCR to measure the transcript levels of protein-coding genes and TEs. Reverse primers used in this study include oligo(dT), random DNA oligos, and sequence-specific DNA oligos. ReverTra Ace qPCR RT Master Mix with gDNA remover (FSQ301; Toyobo) was used for reverse transcription. For quantitative RT-PCR, SYBR Premix Ex Taq II (Tli RNaseH Plus) (RR420A; Takara) was used on an

Applied Biosystems 7500 Fast real-time PCR system. The RNA transcript levels were determined by three independent biological replicates. RNA transcripts were also subjected to RT-PCR and examined on ethidium bromide–stained agarose gels; the gel-based RT-PCR results were confirmed by quantitative RT-PCR in this study. The primer sequences are listed in Supplemental Data Set 8 online. *ACT7* was used as an internal control. To confirm the absence of DNA contamination in the RNA samples, we amplified *ACT7* by directly using RNA as templates. The amplification was shown as "No RT." The absence of amplification indicated the absence of DNA contamination.

DNA Methylation Analysis

DNA methylation was analyzed by bisulfite sequencing, DNA gel blotting, and chop-PCR. For bisulfite sequencing, 2 μg of genomic DNA was treated and purified according to the protocol for the EpiTect bisulfite kit (Qiagen). The purified DNA was amplified, and the amplification product was cloned into the pMD18-T vector (Takara) for sequencing. The DNA methylation levels at CG, CHG, and CHH sites were separately calculated. For DNA gel blotting, genomic DNA was cleaved with the DNA methylation-sensitive endonucleases *Hpa*II, *Msp*I, and *Hae*III at 37°C for 2 d and run on 1% agarose gels. The probes of 180-bp centromeric DNA repeats, *TSI*, and *5S rDNA* were labeled by [α-^{32}P]dCTP with Klenow enzyme. The endonuclease *Mcr*BC cleaves DNA containing methylated cytosine but has no action on unmethylated DNA. For chop-PCR, genomic DNA was cleaved with McrBC, and the products were subjected to PCR and quantitative PCR.

Whole-Genome Bisulfite Sequencing

Raw sequencing data was mapped to TAIR10 reference genome modified by the single nucleotide polymorphisms between C24 and Columbia-0. Only the sequences mapped to unique positions on the *Arabidopsis* genome were retained for DNA methylation analysis. DNA methylation was calculated when cytosine sites have at least fivefold coverage. The methylation level for each cytosine was evaluated by the percentage of reads reporting a C in the total number of reads at the site. Gene and TE annotations were downloaded from The Arabidopsis Information Resource. One-kilobase upstream and downstream surrounding regions were included to calculate the DNA methylation levels of genes and TEs. The methylation levels of genes and TEs were estimated by pooling the read counts that show at least fivefold coverage. CG, CHG, and CHH methylation was calculated.

Annotated genes or transposons including 1-kb upstream and downstream flanking sequences were aligned to the modified TAIR10 reference genome. The average methylation level for each 100-bp interval was plotted. The lengths of genes or transposons were adjusted to a common sum. DNA methylation levels in 200-kb windows were plotted across each chromosome to indicate the genome-wide DNA methylation status in *ros1*, *ros1 fpgs1*, and *ros1 ddm1*. The fold change of DNA methylation between *ros1 fpgs1* and *ros1* in the 200-kb window was calculated and shown across each chromosome. To evaluate the correlation between differentially expressed genes or TEs and DNA methylation, we determined the DNA methylation levels of different classes of differentially expressed genes and TEs using the method described previously (Zhang et al., 2013).

Immunofluorescence Assay

Histone H3K9 dimethylation was immunolocalized as previously described (Onodera et al., 2005). In brief, after nuclei were blocked with 3% BSA in PBS, the primary antibody H3K9me2 (ab1220; Abcam) was diluted at 1:50 and incubated overnight at 4°C. Secondary anti-mouse fluorescein isothiocyanate (Invitrogen) or anti-rabbit fluorescein isothiocyanate (Invitrogen) was used at 1:200 dilutions and incubated for 2 h at 37°C. Chromatin was counterstained with 4′,6-diamidino-2-phenylindole in mounting medium. Images were acquired with a spinning-disk confocal microscope and processed with Adobe Photoshop (Adobe).

RNA Deep Sequencing and Data Analysis

Total RNA was extracted from 2-week-old *Arabidopsis* seedlings and sent to Beijing Genomics Institute for RNA library preparation and deep sequencing. *Arabidopsis* genome sequences and annotated gene models were downloaded from TAIR10 (http://www.Arabidopsis.org/). Tophat v2.0.6 was used to align the raw RNA reads to the *Arabidopsis* genome (Trapnell et al., 2009), allowing up to two mismatches. The edgeR package (Robinson et al., 2010) was used in the differential expression analysis for genes and TEs. Significance of expression differences was calculated using Fisher's exact test. The distribution of differentially expressed genes and TEs throughout the *Arabidopsis* genome was plotted by circos (Krzywinski et al., 2009).

Measurement of Metabolites in *Arabidopsis* Seedlings

Two-week-old *Arabidopsis* seedlings from MS medium plates were used for measurement of SAM, SAH, Hcy, Cys, and Met. The methods for sample preparation and metabolite measurement were previously described (Nikiforova et al., 2005). The experiments were biologically repeated three times.

Accession Numbers

Sequence data from this article can be found in the Arabidopsis Genome Initiative or GenBank/EMBL databases under the following accession numbers: AT5G66750 (*DDM1*), AT5G05980 (*FPGS1*), AT3G10160 (*FPGS2*), AT3G55630 (*FPGS3*), AT4G13940 (*HOG1*), AT2G36490 (*ROS1*), AT5G49160 (*MET1*), AT5G52310 (*RD29A*), AT2G17690 (*SDC*), At4g03650 (At-*GP1*), At4g08680 (*AtMU1*), BD298459.1 (*TSI*), and AT5G09810 (*ACT7*).

Supplemental Data

The following materials are available in the online version of this article.

Supplemental Figure 1. Identification and Characterization of *DDM1*.

Supplemental Figure 2. Quantitative RT-PCR of *NPTII*, *SDC*, *TSI*, *AtMU1*, and *AtGP1*.

Supplemental Figure 3. The Effect of *fpgs1* and *ddm1* on DNA Methylation.

Supplemental Figure 4. Identification and Characterization of *FPGS1*.

Supplemental Figure 5. Identification of Abnormal *FPGS1* Transcript Variants in *ros1 fpgs1* Compared with That in the Wild Type and *ros1*.

Supplemental Figure 6. Complementation Assay for *fpgs1*.

Supplemental Figure 7. DNA Methylation and Transcriptional Silencing in the T-DNA *fpgs1*, *fpgs2*, and *fpgs3* Mutants.

Supplemental Figure 8. The Effect of *fpgs1* and *ddm1* on DNA Methylation at the Promoters of the *35S-NPTII* and *RD29A-LUC* Transgenes.

Supplemental Figure 9. The Effect of *fpgs1* and *ddm1* on DNA Methylation across *Arabidopsis* Chromosomes.

Supplemental Figure 10. Quantitative RT-PCR of the Genes and TEs Identified by RNA Deep Sequencing.

Supplemental Figure 11. The DNA Methylation Levels of *fpgs1* Upregulated Genes and TEs Were Determined by Chop-PCR.

Supplemental Figure 12. The Effect of 5-CHO-THF on DNA Methylation at 180-bp Centromeric DNA and *TSI* Sites in the Wild type, *ros1*, and *ros1 fpgs1*.

Supplemental Table 1. Primary Data for Locus-Specific Bisulfite Sequencing.

Supplemental Table 2. Numbers of Obtained Reads from Whole-Genome Bisulfite Sequencing.

Supplemental Table 3. Numbers of Obtained RNA Reads from RNA Deep Sequencing.

Supplemental Data Set 1. Differentially Methylated Genes Caused by *fpgs1*.

Supplemental Data Set 2. Differentially Methylated Transposable Elements Caused by *fpgs1*.

Supplemental Data Set 3. Differentially Methylated Genes Caused by *ddm1*.

Supplemental Data Set 4. Differentially Methylated Transposable Elements Caused by *ddm1*.

Supplemental Data Set 5. List of Differentially Expressed Genes Affected by *fpgs1*.

Supplemental Data Set 6. List of Differentially Expressed Transposable Elements Affected by *fpgs1*.

Supplemental Data Set 7. List of AGI Annotated Genes and Transposable Elements Upregulated by *fpgs1*.

Supplemental Data Set 8. List of DNA Oligos Used in This Study.

ACKNOWLEDGMENTS

We thank Zhirong Shen at the Metabolomics Center of National Institute of Biological Sciences, Beijing, for technical assistance in metabolite analysis. This work was supported by the National Basic Research Program of China (973 Program; 2012CB910900) and the 973 Program (2011CB812600) from the Chinese Ministry of Science and Technology.

AUTHOR CONTRIBUTIONS

H.-R.Z. performed research, analyzed the data, and wrote the article. F.-F.Z. performed research and analyzed the data. Z.-Y.M. and L.J. performed research. H.-W.H., T.C., J.-K.Z., and C.Z. analyzed the data. X.-J.H. designed the research, analyzed the data, and wrote the article.

Received June 9, 2013; revised June 9, 2013; accepted July 10, 2013; published July 23, 2013.

REFERENCES

Bacolla, A., Pradhan, S., Roberts, R.J., and Wells, R.D. (1999). Recombinant human DNA (cytosine-5) methyltransferase. II. Steady-state kinetics reveal allosteric activation by methylated DNA. J. Biol. Chem. **274:** 33011–33019.

Baubec, T., Dinh, H.Q., Pecinka, A., Rakic, B., Rozhon, W., Wohlrab, B., von Haeseler, A., and Mittelsten Scheid, O. (2010). Cooperation of multiple chromatin modifications can generate unanticipated stability of epigenetic states in *Arabidopsis*. Plant Cell **22:** 34–47.

Baumbusch, L.O., Thorstensen, T., Krauss, V., Fischer, A., Naumann, K., Assalkhou, R., Schulz, I., Reuter, G., and Aalen, R.B. (2001). The *Arabidopsis thaliana* genome contains at least 29 active genes encoding SET domain proteins that can be assigned to four evolutionarily conserved classes. Nucleic Acids Res. **29:** 4319–4333.

Cao, X., and Jacobsen, S.E. (2002). Locus-specific control of asymmetric and CpNpG methylation by the DRM and CMT3 methyltransferase genes. Proc. Natl. Acad. Sci. USA **99** (Suppl 4)**:** 16491–16498.

Cossins, E.A., and Chen, L. (1997). Folates and one-carbon metabolism in plants and fungi. Phytochemistry **45:** 437–452.

Du, J., et al. (2012). Dual binding of chromomethylase domains to H3K9me2-containing nucleosomes directs DNA methylation in plants. Cell **151:** 167–180.

Friso, S., Choi, S.W., Girelli, D., Mason, J.B., Dolnikowski, G.G., Bagley, P.J., Olivieri, O., Jacques, P.F., Rosenberg, I.H., Corrocher, R., and Selhub, J. (2002). A common mutation in the 5,10-methylenetetrahydrofolate reductase gene affects genomic DNA methylation through an interaction with folate status. Proc. Natl. Acad. Sci. USA **99:** 5606–5611.

Frosst, P., et al. (1995). A candidate genetic risk factor for vascular disease: A common mutation in methylenetetrahydrofolate reductase. Nat. Genet. **10:** 111–113.

Giovannucci, E., Stampfer, M.J., Colditz, G.A., Rimm, E.B., Trichopoulos, D., Rosner, B.A., Speizer, F.E., and Willett, W.C. (1993). Folate, methionine, and alcohol intake and risk of colorectal adenoma. J. Natl. Cancer Inst. **85:** 875–884.

Gong, Z., Morales-Ruiz, T., Ariza, R.R., Roldan-Arjona, T., David, L., and Zhu, J.K. (2002). ROS1, a repressor of transcriptional gene silencing in *Arabidopsis*, encodes a DNA glycosylase/lyase. Cell **111:** 803–814.

He, X.J., Chen, T., and Zhu, J.K. (2011). Regulation and function of DNA methylation in plants and animals. Cell Res. **21:** 442–465.

He, X.J., Hsu, Y.F., Pontes, O., Zhu, J., Lu, J., Bressan, R.A., Pikaard, C., Wang, C.S., and Zhu, J.K. (2009). NRPD4, a protein related to the RPB4 subunit of RNA polymerase II, is a component of RNA polymerases IV and V and is required for RNA-directed DNA methylation. Genes Dev. **23:** 318–330.

He, X.J., Hsu, Y.F., Zhu, S., Wierzbicki, A.T., Pontes, O., Pikaard, C.S., Liu, H.L., Wang, C.S., Jin, H., and Zhu, J.K. (2009b). An effector of RNA-directed DNA methylation in *Arabidopsis* is an ARGONAUTE 4- and RNA-binding protein. Cell **137:** 498–508.

Henderson, I.R., Deleris, A., Wong, W., Zhong, X., Chin, H.G., Horwitz, G.A., Kelly, K.A., Pradhan, S., and Jacobsen, S.E. (2010). The de novo cytosine methyltransferase DRM2 requires intact UBA domains and a catalytically mutated paralog DRM3 during RNA-directed DNA methylation in *Arabidopsis thaliana*. PLoS Genet. **6:** e1001182.

Henderson, I.R., and Jacobsen, S.E. (2008). Tandem repeats upstream of the *Arabidopsis* endogene SDC recruit non-CG DNA methylation and initiate siRNA spreading. Genes Dev. **22:** 1597–1606.

Jeddeloh, J.A., Stokes, T.L., and Richards, E.J. (1999). Maintenance of genomic methylation requires a SWI2/SNF2-like protein. Nat. Genet. **22:** 94–97.

Johnson, L.M., Law, J.A., Khattar, A., Henderson, I.R., and Jacobsen, S.E. (2008). SRA-domain proteins required for DRM2-mediated de novo DNA methylation. PLoS Genet. **4:** e1000280.

Krzywinski, M., Schein, J., Birol, I., Connors, J., Gascoyne, R., Horsman, D., Jones, S.J., and Marra, M.A. (2009). Circos: An information aesthetic for comparative genomics. Genome Res. **19:** 1639–1645.

Law, J.A., and Jacobsen, S.E. (2010). Establishing, maintaining and modifying DNA methylation patterns in plants and animals. Nat. Rev. Genet. **11:** 204–220.

Liu, J., Bai, G., Zhang, C., Chen, W., Zhou, J., Zhang, S., Chen, Q., Deng, X., He, X.J., and Zhu, J.K. (2011). An atypical component of RNA-directed DNA methylation machinery has both DNA methylation-dependent and -independent roles in locus-specific transcriptional gene silencing. Cell Res. **21:** 1691–1700.

Liu, Q., and Gong, Z. (2011). The coupling of epigenome replication with DNA replication. Curr. Opin. Plant Biol. **14:** 187–194.

Loenen, W.A. (2006). S-adenosylmethionine: Jack of all trades and master of everything? Biochem. Soc. Trans. **34:** 330–333.

Lucock, M. (2000). Folic acid: Nutritional biochemistry, molecular biology, and role in disease processes. Mol. Genet. Metab. **71:** 121–138.

Matherly, L.H., and Goldman, D.I. (2003). Membrane transport of folates. Vitam. Horm. **66:** 403–456.

Matzke, M., Kanno, T., Daxinger, L., Huettel, B., and Matzke, A.J. (2009). RNA-mediated chromatin-based silencing in plants. Curr. Opin. Cell Biol. **21:** 367–376.

Mehrshahi, P., et al. (2010). Functional analysis of folate polyglutamylation and its essential role in plant metabolism and development. Plant J. **64:** 267–279.

Molloy, A.M. (2012). Genetic aspects of folate metabolism. Subcell. Biochem. **56:** 105–130.

Mull, L., Ebbs, M.L., and Bender, J. (2006). A histone methylation-dependent DNA methylation pathway is uniquely impaired by deficiency in *Arabidopsis* S-adenosylhomocysteine hydrolase. Genetics **174:** 1161–1171.

Nikiforova, V.J., Kopka, J., Tolstikov, V., Fiehn, O., Hopkins, L., Hawkesford, M.J., Hesse, H., and Hoefgen, R. (2005). Systems rebalancing of metabolism in response to sulfur deprivation, as revealed by metabolome analysis of *Arabidopsis* plants. Plant Physiol. **138:** 304–318.

Onodera, Y., Haag, J.R., Ream, T., Costa Nunes, P., Pontes, O., and Pikaard, C.S. (2005). Plant nuclear RNA polymerase IV mediates siRNA and DNA methylation-dependent heterochromatin formation. Cell **120:** 613–622.

Ouyang, B., Fei, Z., Joung, J.G., Kolenovsky, A., Koh, C., Nowak, J., Caplan, A., Keller, W.A., Cui, Y., Cutler, A.J., and Tsang, E.W. (2012). Transcriptome profiling and methyl homeostasis of an *Arabidopsis* mutant deficient in S-adenosylhomocysteine hydrolase1 (SAHH1). Plant Mol. Biol. **79:** 315–331.

Rajakumara, E., Law, J.A., Simanshu, D.K., Voigt, P., Johnson, L.M., Reinberg, D., Patel, D.J., and Jacobsen, S.E. (2011). A dual flip-out mechanism for 5mC recognition by the *Arabidopsis* SUVH5 SRA domain and its impact on DNA methylation and H3K9 dimethylation in vivo. Genes Dev. **25:** 137–152.

Ravanel, S., Cherest, H., Jabrin, S., Grunwald, D., Surdin-Kerjan, Y., Douce, R., and Rébeillé, F. (2001). Tetrahydrofolate biosynthesis in plants: Molecular and functional characterization of dihydrofolate synthetase and three isoforms of folylpolyglutamate synthetase in *Arabidopsis thaliana*. Proc. Natl. Acad. Sci. USA **98:** 15360–15365.

Robinson, M.D., McCarthy, D.J., and Smyth, G.K. (2010). edgeR: A Bioconductor package for differential expression analysis of digital gene expression data. Bioinformatics **26:** 139–140.

Rocha, P.S., Sheikh, M., Melchiorre, R., Fagard, M., Boutet, S., Loach, R., Moffatt, B., Wagner, C., Vaucheret, H., and Furner, I. (2005). The *Arabidopsis* HOMOLOGY-DEPENDENT GENE SILENCING1 gene codes for an S-adenosyl-L-homocysteine hydrolase required for DNA methylation-dependent gene silencing. Plant Cell **17:** 404–417.

Ronemus, M.J., Galbiati, M., Ticknor, C., Chen, J., and Dellaporta, S.L. (1996). Demethylation-induced developmental pleiotropy in *Arabidopsis*. Science **273:** 654–657.

Roudier, F., et al. (2011). Integrative epigenomic mapping defines four main chromatin states in *Arabidopsis*. EMBO J. **30:** 1928–1938.

Shane, B. (1989). Folylpolyglutamate synthesis and role in the regulation of one-carbon metabolism. Vitam. Horm. **45:** 263–335.

Shelnutt, K.P., Kauwell, G.P., Gregory, J.F., III., Maneval, D.R., Quinlivan, E.P., Theriaque, D.W., Henderson, G.N., and Bailey, L.B. (2004). Methylenetetrahydrofolate reductase 677C—>T polymorphism affects DNA methylation in response to controlled folate intake in young women. J. Nutr. Biochem. **15:** 554–560.

Slotkin, R.K., and Martienssen, R. (2007). Transposable elements and the epigenetic regulation of the genome. Nat. Rev. Genet. **8:** 272–285.

Sridhar, V.V., Kapoor, A., Zhang, K., Zhu, J., Zhou, T., Hasegawa, P.M., Bressan, R.A., and Zhu, J.K. (2007). Control of DNA methylation and heterochromatic silencing by histone H2B deubiquitination. Nature **447:** 735–738.

Srivastava, A.C., Ramos-Parra, P.A., Bedair, M., Robledo-Hernández, A.L., Tang, Y., Sumner, L.W., Díaz de la Garza, R.I., and Blancaflor, E.B. (2011). The folylpolyglutamate synthetase plastidial isoform is required for postembryonic root development in *Arabidopsis*. Plant Physiol. **155:** 1237–1251.

Tanaka, H., Masuta, C., Uehara, K., Kataoka, J., Koiwai, A., and Noma, M. (1997). Morphological changes and hypomethylation of DNA in transgenic tobacco expressing antisense RNA of the S-adenosyl-L-homocysteine hydrolase gene. Plant Mol. Biol. **35:** 981–986.

Teixeira, F.K., et al. (2009). A role for RNAi in the selective correction of DNA methylation defects. Science **323:** 1600–1604.

To, T.K., et al. (2011). *Arabidopsis* HDA6 regulates locus-directed heterochromatin silencing in cooperation with MET1. PLoS Genet. **7:** e1002055.

Trapnell, C., Pachter, L., and Salzberg, S.L. (2009). TopHat: Discovering splice junctions with RNA-Seq. Bioinformatics **25:** 1105–1111.

Veiseth, S.V., Rahman, M.A., Yap, K.L., Fischer, A., Egge-Jacobsen, W., Reuter, G., Zhou, M.M., Aalen, R.B., and Thorstensen, T. (2011). The SUVR4 histone lysine methyltransferase binds ubiquitin and converts H3K9me1 to H3K9me3 on transposon chromatin in *Arabidopsis*. PLoS Genet. **7:** e1001325.

Wierzbicki, A.T., Cocklin, R., Mayampurath, A., Lister, R., Rowley, M.J., Gregory, B.D., Ecker, J.R., Tang, H., and Pikaard, C.S. (2012). Spatial and functional relationships among Pol V-associated loci, Pol IV-dependent siRNAs, and cytosine methylation in the *Arabidopsis* epigenome. Genes Dev. **26:** 1825–1836.

Wu, X., Li, F., Kolenovsky, A., Caplan, A., Cui, Y.H., Cutler, A., and Tsang, E.W.T. (2009). A mutant Deficient in S-adenosylhomocysteine hydrolase in *Arabidopsis* shows defects in root hair development. Botany **87:** 571–584.

Xia, R., Wang, J., Liu, C., Wang, Y., Wang, Y., Zhai, J., Liu, J., Hong, X., Cao, X., Zhu, J.K., and Gong, Z. (2006). ROR1/RPA2A, a putative replication protein A2, functions in epigenetic gene silencing and in regulation of meristem development in *Arabidopsis*. Plant Cell **18:** 85–103.

Yin, H., Zhang, X., Liu, J., Wang, Y., He, J., Yang, T., Hong, X., Yang, Q., and Gong, Z. (2009). Epigenetic regulation, somatic homologous recombination, and abscisic acid signaling are influenced by DNA polymerase epsilon mutation in *Arabidopsis*. Plant Cell **21:** 386–402.

Zhang, H., Deng, X., Miki, D., Cutler, S., La, H., Hou, Y.J., Oh, J., and Zhu, J.K. (2012). Sulfamethazine suppresses epigenetic silencing in *Arabidopsis* by impairing folate synthesis. Plant Cell **24:** 1230–1241.

Zhang, H., et al. (2013). DTF1 is a core component of RNA-directed DNA methylation and may assist in the recruitment of Pol IV. Proc. Natl. Acad. Sci. USA **110:** 8290–8295.